sustainability

MDPI

Article

Metal Rod Surfaces after Exposure to Used Cooking Oils

Nina Bruun *, Juho Lehmusto, Jarl Hemming, Fiseha Tesfaye and Leena Hupa

Johan Gadolin Process Chemistry Centre, Åbo Akademi University, Henrikinkatu 2, FI-20500 Turku, Finland; juho.lehmusto@abo.fi (J.L.); jarl.hemming@abo.fi (J.H.); fiseha.tesfaye@abo.fi (F.T.); leena.hupa@abo.fi (L.H.)
* Correspondence: nina.bruun@abo.fi

Abstract: Used cooking oils (UCOs) have a high potential as renewable fuels for the maritime shipping industry. However, their corrosiveness during storage and usage are some of the concerns yet to be investigated for addressing compatibility issues. Thus, the corrosion of steels and copper exposed to the UCOs was studied through the immersion of metal rods for different periods. The changes on the rod surfaces were analyzed with a scanning electron microscope (SEM). After the immersion, the copper concentration dissolved in the bio-oils was measured using inductively coupled plasma-optical emission spectrometry (ICP-OES). The free fatty acids and glycerides were analyzed using gas chromatography with flame ionization detection (GC-FID). The acid number (AN), water concentration, as well as density and kinematic viscosity of the bio-oils were determined with standard methods. The UCOs with the highest water content were corrosive, while the oils with lower water concentrations but higher ANs induced lower corrosion. After mixing two different UCOs, the metal corrosion decreased with an increasing concentration of the oil with lower corrosive properties. The lower corrosion properties were most likely due to the monounsaturated fatty acids, e.g., oleic acid in oils. These acids formed a barrier layer on the rod surfaces, thereby inhibiting the permeation of oxygen and water to the surface. Even adding 0.025 wt% of tert-butylamine decreased the corrosivity of UCO against polished steel rod. The results suggested that mixing several oil batches and adding a suitable inhibitor reduces the potential corrosive properties of UCOs.

Keywords: corrosion; inhibitor; used cooking oil; renewable energy sources

Citation: Bruun, N.; Lehmusto, J.; Hemming, J.; Tesfaye, F.; Hupa, L. Metal Rod Surfaces after Exposure to Used Cooking Oils. *Sustainability* **2022**, *14*, 355. https://doi.org/10.3390/su14010355

Academic Editors: Luca Marchitto and Cinzia Tornatore

Received: 14 November 2021
Accepted: 25 December 2021
Published: 29 December 2021

1. Introduction

Used cooking vegetable oils (UCOs) are waste streams and of great interest as renewable fuels. Thus, they neither compete with the food chain nor utilize farmland for their production. These circumstances make UCOs an attractive feedstock for future transportation fuels for maritime shipping, aviation, and material production [1,2]. The current demand of EU and UK for UCOs and UCO-based biodiesel (UCOBD) is 2.8 Mt/y. The maximum worldwide UCO and UCOBD production is predicted to be between 3.1 and 3.3 Mt/y by 2030 [2]. On a global scale, the need for UCOs and UCOBDs is 27–37 Mt/y in 2030 if the projected EU share of UCOBDs in renewable transport fuels is achieved [2].

UCOs are mixtures of triglycerides, diglycerides, monoglycerides, and fatty acids contaminated by derivatives from the food frying process, such as free fatty acids (FFAs), heterocycles, Maillard reaction products, and metal traces originating from pads and food leaching [3–5]. UCOs are also raw materials for other industries, e.g., production of bio-plasticizers, syngas, and sorbents for volatile organic compounds (VOCs) [6–8].

In the utilization of UCOs, corrosivity during storage and usage are some of the concerns yet to be investigated for addressing materials compatibility issues with the UCOs. According to the experimental investigation of Fazal et al. [9], on the surface of metals exposed to biodiesel as well as water and oxygen at room temperature and for different periods, corrosion products consisting of metal-oxides, -carbonates, and -hydroxides can be formed. Figure 1 illustrates the overall phenomena at the interface of a metal and biodiesel as described in literature [9]. Despite the compositional differences between UCO

and biodiesel, the same phenomena depicted in Figure 1 could occur also at metal/UCO interfaces under similar conditions.

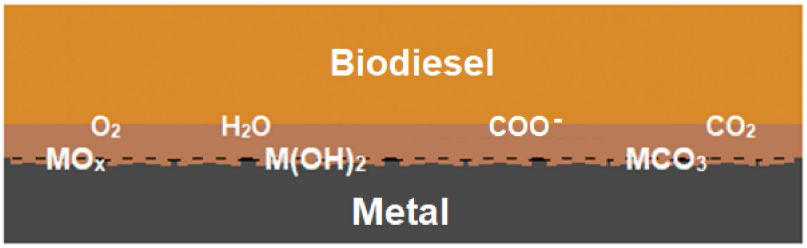

Figure 1. Schematic illustration of the phenomena at the interface of a metal (M) and biodiesel exposed to the atmosphere at room temperature and different periods. COO^{-} represents short-chain radicals formed by breaking down of long-chain molecules.

Corrosion in fuel tanks, fuel injection systems, and deterioration of the hot parts in the exhaust gas stream originates partly from fuel properties [10]. In petroleum production, oxidation leading to corrosion is controlled by antioxidants, while corrosion inhibitors hinder oxidation through adsorption on reactive sites of potentially catalytic metal surfaces forming a monomolecular layer of the functional group that prevents metal contacting directly with the fuel [11]. For example, an eco-friendly formulation of *Opuntia dillenii* seed oil was reported to act as a corrosion inhibitor to protect iron in an acidic environment, such as acid rain [12]. This oil is a significant source of fatty acids, sterols, and vitamin E, which forms a barrier layer on the iron surface and minimize the contact between the metal surface and the corrosive solution [12].

According to Bruun et al. [13], oleic acid or oleic acid and glycerol additions prevented corrosion of steel rods exposed to UCOs. Fazal et al. [14] reported a significant increase in corrosion rate upon immersion of metals in fossil and biodiesel samples at 27 °C, 50 °C, and 80 °C for 50 days. They concluded that the oxidation instability of the oil contributed to the corrosion mechanism. Immersion tests of metal coupons in various diesel-biodiesel mixtures at 43 °C for two months were carried out by Hu et al. [15]. Their results showed that diesel containing biodiesel components led to a tenfold higher corrosion rate than plain fossil diesel. Copper and carbon steel were the most susceptible to corrosion, while stainless steel showed good resistance [15]. Copper has been found to act as a strong catalyst for oxidizing palm biodiesel [16]. Alves et al. [17] reported that small metal ions released during a stainless steel surface corrosion promoted biodiesel oxidation. Accordingly, the fuel quality and its oxidative stability changed.

Natural additives, such as rosmarinic acid, curcumin, and gingerol, have been found to increase the oxidative stability of soybean biodiesel and the corrosion resistance of carbon steel in the oil [18]. Curcumin was found the best additive concerning oxidative stability, while rosmarinic acid showed better performance as a corrosion inhibitor. The effects were related to the presence of phenolic compounds or oxygen in the molecular structures of these compounds [18].

Polar amine groups in amine-based inhibitors have been reported to be capable of ionizing at interfaces and adsorbing heterocyclic moiety via nitrogen atoms, which enhanced corrosion inhibiting properties of metal surfaces [19,20]. Well-known corrosion inhibitors include organic compounds that contain nitrogen, oxygen, or sulfur atoms, heterocyclic compounds, and pi electrons [21]. The polar functional groups present in inhibitors are considered the center of reaction for adsorption [22]. Water content, temperature, microbial growth, and raw material used for biodiesel production influence the corrosion rate. The amount of unsaturated free fatty acid in the raw material for biodiesel production has a high impact on the oxidation rate. The metals commonly used in compression ignition engines, such as copper and copper alloys, steel, and aluminum, are prone to corrosion [23,24]. Inhibitors ethylenediamine, tert-butylamine (TBA), and n-butylamine formed a stable metal oxide protective layer and thus retarded the corrosion in biodiesel [23,25].

In our previous works, the chemical, physical, and thermal properties and the effect of storage time on the corrosivity of bio-oils were investigated [13,26,27]. The corrosiveness of different bio-oils during storage and usage are some of the concerns yet to be investigated for addressing compatibility issues. Thus, the corrosion of steels and copper exposed to the UCOs was studied through the immersion of metal rods for different periods. This work aimed to find out whether different UCO batches have variations in their corrosive properties. Additionally, preliminary studies of the corrosivity of oil mixtures and adding a corrosion inhibitor to the most corrosive batch were carried out.

2. Materials and Methods

Eight freshly processed cooking oils (UCO1–UCO8) collected from fast food companies were received from VG EcoFuel Oy (Uusikaupunki, Finland) and studied in detail. In the abbreviations of the oils, numbers presented different oil batches. All used cooking oils are vegetable-based and filtered. Prior to the experiments, the oils were stored in a refrigerator.

TBA (98%), used as a corrosion inhibitor, was purchased from Sigma-Aldrich (Saint Louis, MO, USA). The other chemicals used for chemical analyses are described in [13,26,27]. All chemicals and solvents used in the experiment were of analytical reagent grade.

Capillary gas chromatography with flame ionization detection (GC-FID) (Perkin Elmer Autosystem XL (Waltham, MA, USA)) was used to quantify the amount of FFAs and monoglycerides in silylated oil samples. The experimental error for this method is estimated to be ±5%. An Agilent J&W HP-1 (Santa Clara, CA, USA), 25 m (L) × 0.200 mm (ID) column with film thickness 0.11 µm was used. Hydrogen was used as a carrier gas with a flow rate of 0.8 mL/min. Details on the oven temperatures and gas flow rates can be found in [13]. The individual components were identified by capillary gas chromatography-mass spectrometry (GC-MS) analysis with a Hewlett-Packard (HP) 6890-5973 GC-quadrupole-MSD instrument (Palo Alto, CA, USA), using helium as carrier gas.

By applying a wide-bore short column GC-FID (PerkinElmer Clarus 500 (Waltham, MA, USA)), di- and triglycerides were analyzed. Dimensions of the column (Agilent HP-1/SIMDIST (Santa Clara, CA, USA)) were 0.15 µm (film thickness) and 6 m (L) × 0.530 mm (ID). Hydrogen was the carrier gas with a flow rate of 7 mL/min. Details of the temperatures in a wide-bore GC oven and gas flow rates can be found in our previous study [13].

Karl Fischer (KF) titration with an automatic coulometric titrator (Metrohm 851 Titrando instrument (Herisau, Appenzell Ausserrhoden, Switzerland)) connected to an oven (860 KF Thermoprep (Herisau, Appenzell Ausserrhoden, Switzerland)) was used to determine the water content of the oils. In the measurements, 100 mg of the sample sealed in a glass tube was studied. The KF measurements were performed under a dry N2 gas atmosphere flowing with a rate of 90 mL/min. The water release of the UCOs was measured at 110 °C three times for each sample.

ASTM D 664 method using Metrohm 888 Titrando (Herisau, Appenzell Ausserrhoden, Switzerland) titrator with the Solvotrode glass electrode (Affoltern, Zürich, Switzerland) was applied to measure the acid number (AN) of the UCOs. Samples of the bio-oils were dissolved in 125 mL of a solution of toluene, propan-2-ol, and deionized water (500:495:5 $v/v/v$) and then titrated with 0.1 M KOH in propan-2-ol. The amount of KOH in propan-2-ol was determined by titration of potassium hydrogen phthalate. The blank test was carried out three times. The theoretical AN was calculated according to a previous study, where the GC analysis results of the total FFA concentrations were converted to theoretical ANs, mg KOH/g oil [27].

The density of all the samples was measured at 21 °C using a 100 mL pycnometer (Wertheim, Baden-Württemberg, Germany). The kinematic viscosity was measured using a Cannon–Fenske (reverse flow) viscometer (Hofheim am Taunus, Hesse, Germany), capillary 51120, using the ASTM D 2515 method in a thermostatic bath at 40 ± 0.5 °C. Three analyses for each sample were performed.

2.1. Experimental Setup and Procedure

2.1.1. Immersion Test

An immersion test was applied at room temperature to investigate the corrosive behavior of UCOs in contact with steels and copper rods. The experiments were performed in test tubes of 15 mL mounted on a rotary mixer rotated at a constant speed of 56 rpm. The rod was placed in a 7-mL oil sample, and the test was conducted over a period of 1, 3, 5, and 10 days (1 d, 3 d, 5 d, and 10 d). During the experiments, the samples were wrapped with duct tape to avoid exposure to light. After the immersion test, the rod was removed from the oil and cleaned ultrasonically using a mixture of toluene and 2-propanol (1:1 v/v). The oils from each experiment were subjected to liquid-liquid extraction using 1 mL of sulfuric acid (95%) and 8 mL of deionized water in a test tube, then vigorously shaken for 1 min. After the extraction, the mixture was filtered using WhatmanTM quantitative filter paper grade No 42 (ashless, Whatman International Ltd., Maidstone, UK), and the aqueous solution was taken for subsequent spectrophotometric analysis. Each experiment was repeated in triplicates.

The polished rods were used to maximize the interaction between the oil and the surface, thus giving us a good starting point to study corrosion. Unpolished samples were used to mimic real-life situation. Mild-annealed steel was used to study the effect of alloying on corrosion resistance.

The capability of the corrosion inhibitor TBA to suppress the corrosivity of bio-oils was investigated using a polished steel rod exposed to three different concentrations of TBA in UCO2 for three days.

Copper was chosen for the immersion test, as it is used in internal combustion engine systems, and gaskets utilize copper-based alloys and copper, respectively [24]. According to [28], copper may oxidize biodiesel and generate sediments.

2.1.2. Metal Rods

The steel rod (98.64 wt% Fe, 1.00 wt% Mn, 0.21 wt% Si, 0.11 wt% C, 0.03 wt% P, and 0.02 wt% S) used in the immersion tests was a H44 all-round welding rod with a diameter of 1.6 mm, obtained from AGA (Finland). The mild annealed steel rod (98.79 wt% Fe, 1.0 wt% Mn, 0.15 wt% Si, and 0.06 wt% C) and the copper rod (99.9 wt% Cu) had 1.5 and 1.0 mm diameters, respectively. All rods were cut in 85-mm long pieces, and the ends were polished to a similar roughness (visually) as the surfaces of the rod.

Surface polishing of the steel rod was carried out to standardize the starting point for the experiments. The surface was polished first with grinding paper Buehler CarbiMetTM, Grit 280 [P320], and then with Buehler-Met® II, Silicon Carbide grinding paper, Grit 360 [P600].

2.1.3. Dissolved Metal Ions in Oils

The amount of iron dissolved in oils during the experiment was determined using a spectrophotometer (Perkin-Elmer Lambda 25 (Waltham, MA, USA)) by analyzing the amount of total dissolved iron in the aqueous phase after the liquid-liquid extraction step. The spectra were measured between 400 and 600 nm with a scan rate of 480 nm·min^{-1} using a quartz cuvette with a one cm path length.

After the immersion tests with copper rods, dissolved copper in the bio-oils was measured using inductively coupled plasma-optical emission spectrometry (ICP-OES, Perkin Elmer Optima 5300 DV (Waltham, MA, USA)). HNO_3 (65%) and H_2O_2 were added to digest the sample in a microwave oven (Anton Paar, Multiwave 3000 (Graz, Styria, Austria)). Three analyses were performed of each immersion solution.

2.1.4. Metal Surface Morphology after Oil Exposure

The corrosion on the surfaces of the steel, mild annealed steel, and copper rods was analyzed with a scanning electron microscopy (SEM) LEO Gemini 1530 (Oberkochen,

Baden-Württemberg, Germany) with a Thermo Scientific Ultra Dry Silicon Drift Detector—SDD (Madison, WI, USA).

3. Results and Discussion

3.1. Physicochemical Properties

3.1.1. Diglycerides, Free Fatty Acids, and Monoglycerides

First, the differences in the contents of diglycerides, FFAs, and monoglycerides of the eight UCOs were analyzed. There were no big differences in the amounts of diglycerides (mean value 6.9%), FFAs (mean value 3.3%), and monoglycerides (mean value 0.3%). The rest of the analyzed compounds were triglycerides. The mean value and variations of the saturated and unsaturated free fatty acids and monoglycerides are given in Table 1. Detailed composition of the total FFAs of the UCOs can be found in Table 2. The total FFA values were significantly elevated, especially for UCO8 and UCO5 and probably also for UCO4 (assuming the normal FFA level between 27–28.4 mg/g (Table 2)) since the differences were bigger than 5%. The total FFA values and the AN values (Table 3) indicate similar trends consistently. The unsaturated fatty acid, oleic acid (9-18:1), was 21.7 mg/g in UCO8 and 18.7 mg/g in UCO5. In UCO4, oleic acid was analyzed to be 16.9 mg/g.

Table 1. Total FFA, total saturated FFA, total unsaturated FFA, and total monoglycerides in UCO1-UCO8 samples with capillary column GC-FID.

GC Analysis	Mean Value (mg/g)
Total saturated FFA	3.5 ± 0.7
Total unsaturated FFA	26.6 ± 3.6
Total monoglycerides	1.6 ± 0.6
Total FFA	30.1 ± 3.6

Table 2. Composition of used cooking oil samples UCO1–UCO8 measured with gas chromatography (mg/g oil). n.d. is not detected.

Analyzed Compositions	UCO1	UCO2	UCO3	UCO4	UCO5	UCO6	UCO7	UCO8
Saturated FFA								
C14:0	0.06	0.06	0.04	0.04	0.05	0.05	0.04	0.06
C16:0	1.88	1.82	1.71	1.79	1.80	1.73	1.65	2.14
C17:0	0.07	0.04	0.06	0.07	0.05	0.04	0.07	0.04
C18:0	2.10	2.21	0.72	0.77	0.82	0.72	0.72	0.92
C20:0	0.24	0.25	0.22	0.24	0.26	0.20	0.23	0.28
C22:0	0.19	0.19	0.15	0.16	0.20	0.16	0.15	0.18
Unsaturated FFA								
C16:1	0.07	0.09	0.09	0.08	0.09	0.08	0.08	0.09
C18:3	1.34	1.27	1.57	1.66	1.81	1.48	1.50	2.06
C18:2	5.33	5.41	6.09	6.48	7.20	5.91	6.24	8.36
9-18:1	14.9	14.8	16.0	16.9	18.7	15.24	15.93	21.71
11-18:1	1.84	1.82	1.10	1.20	1.24	0.94	0.97	1.32
cis-13-21:1	0.22	0.24	0.29	0.31	0.35	0.29	0.27	0.40
C20:5	n.d.	n.d.	0.10	0.08	0.10	0.02	0.04	0.03
cis-22:1	0.20	0.22	0.17	0.19	0.18	0.10	0.14	0.20
Monoglycerids								
MG(1)	0.10	0.11	0.11	0.17	0.16	0.08	0.17	0.27
MG(2)	0.29	0.28	0.36	0.41	0.54	0.19	0.40	0.65
MG(3)	0.89	0.88	1.02	1.11	1.49	0.50	1.11	1.67

Table 2. *Cont.*

Analyzed Compositions	UCO1	UCO2	UCO3	UCO4	UCO5	UCO6	UCO7	UCO8
Sterols								
cholesterol	0.13	0.10	0.20	0.10	0.11	0.15	0.08	0.11
farnesol	0.18	0.20	0.19	0.19	0.17	n.d.	n.d.	n.d.
campesterol	0.41	0.42	0.44	0.42	0.41	0.43	0.41	0.38
sitosterol	0.70	0.72	0.71	0.64	0.66	0.71	0.72	0.67
sitostanol	0.06	0.06	0.06	0.03	0.05	0.05	0.05	0.06
Total saturated FFA	4.55	4.58	2.90	3.07	3.18	2.91	2.85	3.61
Saturated FFA/Total FFA	16.0%	16.1%	10.3%	10.2%	9.7%	10.8%	10.2%	9.6%
Total unsaturated FFA	23.9	23.8	25.4	26.9	29.7	24.0	25.2	34.2
Total monoglycerides	1.28	1.28	1.49	1.69	2.19	0.77	1.68	2.58
Total FFA	28.4	28.4	28.3	30.0	32.9	27.0	28.0	37.8

Table 3. Water content, theoretical and measured acid numbers, and concentration of Fe in oils after immersing polished iron rods for three days. The values are averages of three parallel measurements.

Sample	Water Content	Theoretical AN	Measured AN	Immersion Test (3 d)
	(ppm)	(mg KOH/g Oil)	(mg KOH/g Oil)	Fe (ppm)
UCO1	1850	5.7	6.9	12
UCO2	1776	5.7	6.5	389
UCO3	2180	5.6	6.9	102
UCO4	2067	6.0	7.0	14
UCO5	2493	6.5	8.0	74
UCO6	3748	5.4	6.7	449
UCO7	3089	5.6	6.9	571
UCO8	2664	7.5	8.8	59
		Mean value		
UCO1–UCO8	2483	6	7.2	209

3.1.2. Water Content

The water content of the oils is given in Table 3. In general, the water content of only two oils was less than the specification limit, 0.2% v/v [10] for marine engines. FFAs attract water molecules because of their hygroscopic properties. Additionally, mono- and di-glycerides also bind water into vegetable oil fuels [29,30]. Thus, corrosion of the equipment and tanks during the storage can occur if using such oils [26,31]. Therefore, high water content should be taken into account, and strategies for dewatering in tanks should be planned. It was noticed that the visual appearance of the bio-oils (UCO3-UCO8) with a water content >2000 ppm was turbid, while the oils with water content below 2000 ppm looked clear.

3.1.3. Theoretical Acid Number

The theoretical ANs (mg KOH/g oil) were calculated according to Equation (1), and the values are shown in Table 3. When analyzing the total FFA concentrations, no volatile fatty acids, like formic or propionic acids, were detected. These compounds are sometimes added as preservatives to bio-oils [27].

$$\mathrm{AN}\left(\frac{\text{mg KOH}}{\text{g}}\text{oil}\right) = [\text{Total FFA}]\left(\frac{\text{mmol}}{\text{g}}\right).56.1\ \text{mg KOH/mmol} \quad (1)$$

3.1.4. Measured Acid Number

The average measured ANs are shown in Table 3. For all oils, the measured values were higher than the calculated theoretical values. The difference can partly depend on volatile fatty acids not seen in the FFA measurement.

Although UCO8 showed high AN values and relatively high water content, the concentration of dissolved iron was low. Considering that AN value < 5 mg KOH/g oil

implies a minimal corrosion risk, all the oils should have induced some corrosion [10]. On the other hand, the AN values were well below the 15 mg KOH/g oil, a limit set by the engine manufacturers. Notably, the highest concentrations of iron in oils (UCO6 and UCO7) correlate with water contents. In contrast, UCO2 had a low water content and intermediate acid number but showed a relatively high concentration of iron after the immersion test. This implies that the corrosive properties cannot directly be correlated with the water content and acid number.

3.1.5. Density and Kinematic Viscosities of the Bio-Oils

The densities of the UCO1–UCO8 samples analyzed at 21 °C varied only slightly with the average value of 916 ± 1.3 kg/m^3, which is lower than the density of water, 998 kg/m^3. According to the marine diesel engines manufacturer, the density of the liquid biofuel for four-stroke engines should be lower than 991 kg/m^3 [10].

The kinematic viscosities of UCO1-UCO8 analyzed at 40 ± 0.5 °C showed only slight variations with an average value of 39.4 ± 0.3 mm^2/s. The higher kinematic viscosity values of the UCOs compared to a refined commercial product (9.1 mm^2/s) could be due to impurities like starch, polymerized triglycerides, and meat traces [26].

3.2. Corrosion of the Metal Surfaces

3.2.1. Iron-Based Rods

Iron concentration dissolved from the unpolished reference steel rod surfaces into UCO2 increased during the test from 58 ppm (1 d), 84 ppm (3 d), 308 ppm (5 d) to 370 ppm (10 d) (see Figure 2). The values are averages of three parallel samples. For polished steel rod, the iron concentration dissolved into UCO2 first increased up to 5 d (406 ppm) but then decreased to 351 ppm at 10 days. A similar increasing trend during the five first days followed by a lower concentration at 10 days was measured for mild annealed polished steel rods in UCO2. In general, lower ion concentrations were measured for the mild annealed steel rods than for the polished steel rods.

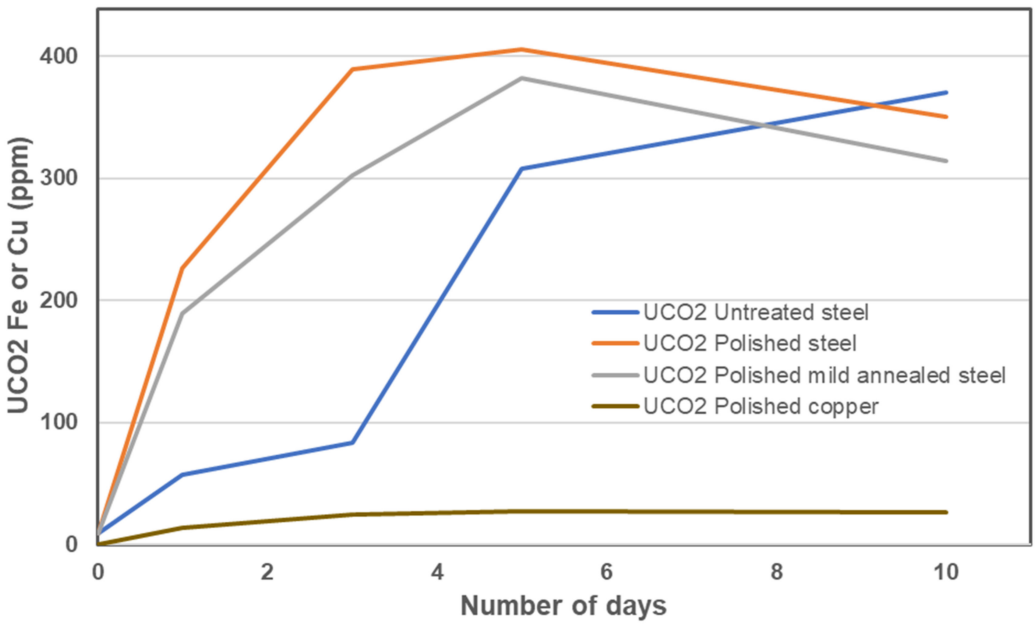

Figure 2. Changes in iron and copper concentrations dissolved from untreated and polished steel rods, polished mild annealed steel rods, and polished copper rods into UCO2 as a function of exposure time. The cumulative error for the measured values is 3%.

For the polished samples, the dissolved iron concentration increased up to five days, after which the amount of dissolved iron started slowly decreasing. The decrease suggested

formation of iron-containing precipitates. This was, however, not verified. Unlike the polished samples, iron continued dissolving from the untreated steel rod, probably because the dissolved iron concentration did not reach saturation during the experiment. No precipitates could be verified on the rod surfaces nor in oils.

The SEM secondary electron images in Figure 3 show the surface morphology of an untreated steel rod, a polished steel rod, and a polished annealed steel rod. The unpolished steel, polished steel, and polished mild anneal steel rod surfaces are shown in Figure 3A–C. The surface morphology of the steel rods is rather even before corrosion. However, polishing gives steep scratches on the surfaces. After immersion for 10 days, the surface morphologies are smoother (Figure 3D–F). As seen in the SEM images, the oil exposure clearly affected the surface morphology of rods, thus suggesting corrosion. This is in agreement with the measured ion concentration in the oil after the exposure.

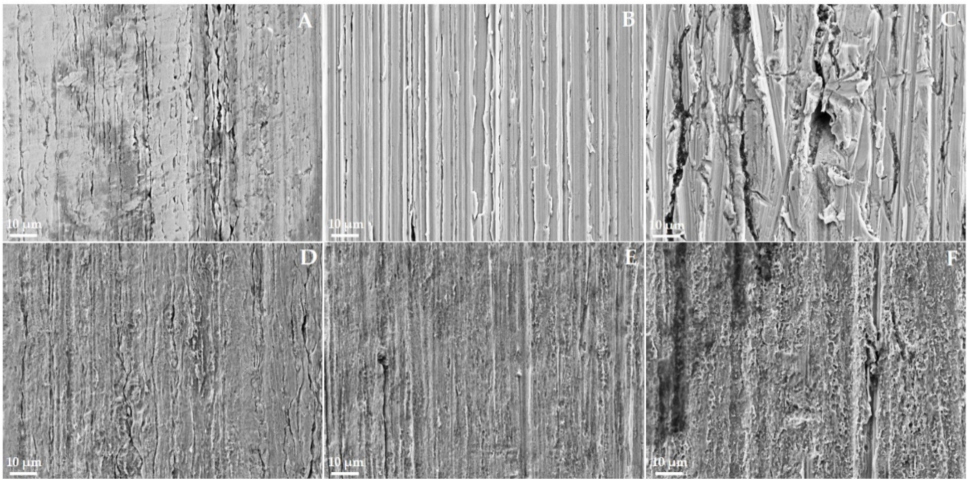

Figure 3. SEM images before oil exposure of (**A**) untreated steel, (**B**) polished steel, and (**C**) polished mild annealed steel. SEM images after 10 days of exposure to UCO2 (**D**) untreated steel, (**E**) polished steel, and (**F**) polished mild annealed steel.

- Iron Concentrations Dissolved from the Rods

Table 4 shows the relative concentrations of iron dissolved from polished steel rods into the different oil batches at different time points. If the measured concentration was less than 50 ppm, the dissolution was considered low (L). Again, concentrations higher than 200 ppm indicated high dissolution (H), while the concentration in between was considered as medium dissolution (M). The average iron concentration in the oils before the exposures was around 8 ppm. UCO1 and UCO4 dissolved a very low iron concentration (8–14 ppm); the reason for this could be that their water concentration is the lowest, and FFAs concentration is among the highest. UCO3, UCO5, and UCO8 dissolved a medium iron concentration (50–199 ppm). The water concentrations were between 2200–2700 ppm, and the ANs were highest compared to the other oils.

Table 4. Relative iron dissolution from polished steel rods into different UCO batches. L, low (8–49 ppm); M, medium (50–199 ppm); H, high (200–600 ppm); n.a., not analyzed.

No. of Days	UCO1	UCO2	UCO3	UCO4	UCO5	UCO6	UCO7	UCO8
1d	L	H	M	n.a.	M	n.a.	n.a.	n.a.
3d	L	H	M	L	M	H	H	M
5d	L	H	L	n.a.	M	n.a.	n.a.	n.a.
10d	L	H	L	n.a.	M	n.a.	n.a.	n.a.

UCO2, UCO6, and UCO7 dissolved a high iron concentration (200–600 ppm). For UCO6 and UCO7, the water content was the highest, between 3100–3750 ppm, and for UCO2, the water content was 1800 ppm, which was also close to the maximum approved level of 2000 ppm of water in oil [10]. The ANs were 6.5–6.9 mg KOH/g oil, which was lower compared to UCO5 and UCO8 samples' ANs (8–8.8 mg KOH/g oil).

The immersion test for three days with a polished steel rod showed higher corrosivity of UCO2, UCO6, and UCO7 (200–600 ppm) but the medium level of corrosivity (50–199 ppm) with UCO3, UCO5, and UCO8 (see Figure 4). In contrast, UCO1 and UCO4 showed the lowest corrosivity (8–49 ppm).

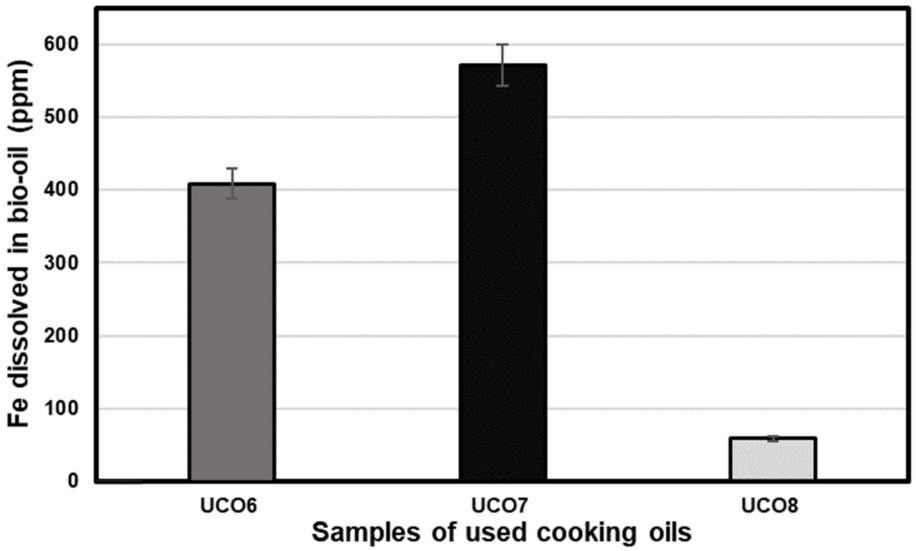

Figure 4. Iron concentration in UCO6, UCO7, and UCO8 after three days in contact with polished steel rods.

Results of the immersion test for all UCO samples for the three days are presented in Table 3 together with the corresponding values for AN and water contents. As the immersion test results presented in Table 3 show that the corrosion properties of these oils (UCO8, UCO5, and UCO4) were lowest compared to the other oils, it could be possible that unsaturated FFAs, e.g., oleic acid, acts as a surfactant on the steel surface and decreases the corrosive properties of UCO oils, as was noticed in a previous study [13]. Fatty acids, such as oleic acid, linoleic acid, and linolenic acid derivatives, are environmentally-friendly corrosion inhibitors protecting mild steel, etc. [32]. Oleic acid was used as a surfactant and bonded covalently to the surfaces of magnetite nanoparticles [33]. A seed oil, *Opuntia dillenii*, which consists of fatty acids, was shown to form a barrier layer on the surface of iron by preventing contact of the metal surface and the corrosive solution [12].

- Exposure to Different UCO Mixtures

The more corrosive UCO2 was mixed with the low corrosive UCO4 in fractions of 9:1, 8:2, 7:3, and 1:1. The immersion test during 3 d with a polished steel rod was implemented. Three replications for each sample were performed. Figure 5 shows the iron concentrations dissolved in the oils. When UCO2 was used in the immersion test, an average iron concentration of 277 ppm was dissolved. As the fractions with decreasing concentration of UCO2 were tested, the concentration of dissolved iron in oil also decreased. The results show that by adding the low corrosive UCO4 oil to a very corrosive UCO2 oil, the harmful corrosive properties of the bio-oil mixture decreased. For utilization of different UCO batches, it would be very important to know the quality of each batch. The most corrosive batches should be blended with the less corrosive batches in a certain proportion such that the influence of the more corrosive oils is minimized.

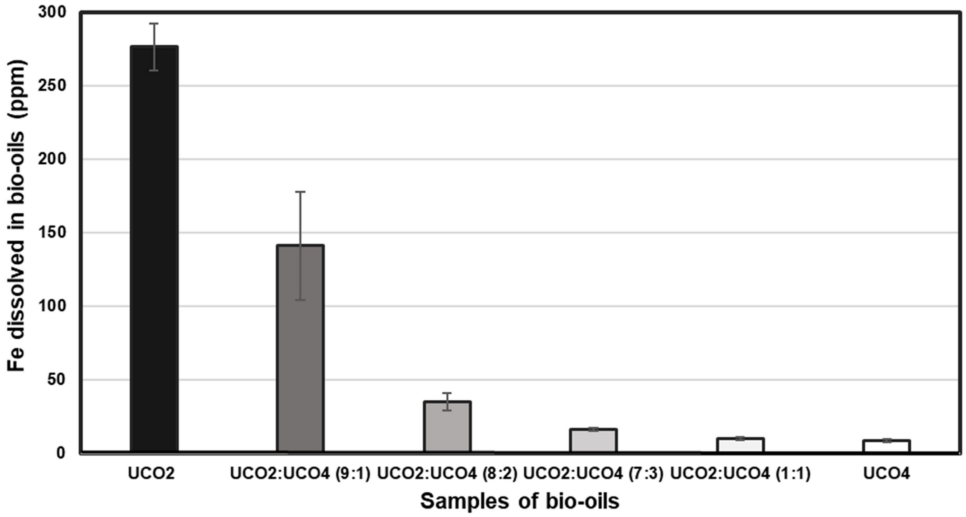

Figure 5. Iron concentration dissolved from polished steel rods into various mixtures of UCO2 and UCO4.

The SEM secondary electron images in Figure 6 show the surface morphology of the polished steel rods after three days of exposure to the following oil samples: (a) UCO2, (b) UCO2:UCO4 (9:1), (c) UCO2:UCO4 (8:2), and (d) UCO4. Figure 6a shows corrosion on the steel surface, 6b shows corrosion, and Figure 6c shows corrosion on the steel surface. Figure 6d shows a very smooth surface with very low corrosion.

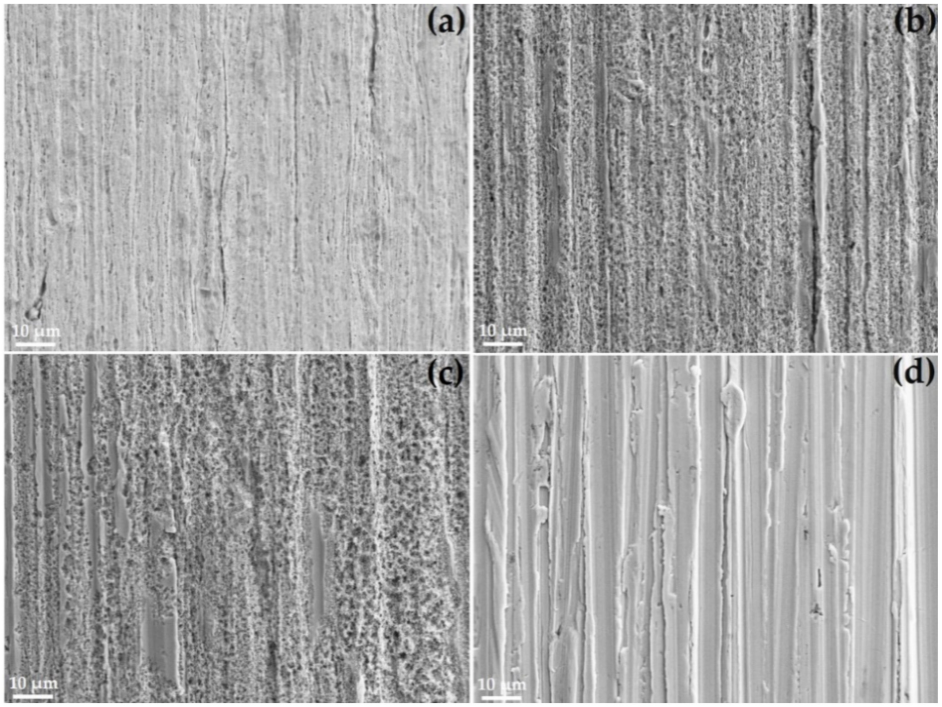

Figure 6. SEM secondary electron images of polished steel rod surfaces after 3 days of exposure to: (**a**) UCO2, (**b**) UCO2:UCO4 (9:1), (**c**) UCO2:UCO4 (8:2), and (**d**) UCO4.

As seen in the SEM images, the oil exposure clearly affected the surface morphology of rods, thus suggesting corrosion. The measured ion concentration in the oil after the exposure also supports this finding.

3.2.2. Copper Rod Corrosion

A polished copper rod was used in the immersion test. The concentration of copper in UCO2 was analyzed with ICP-OES. UCO2 dissolved copper during 1 d only 14 ppm, and during 3 d, 5 d, and 10 d, the level of dissolved copper was 25.9 ± 0.7 ppm (Table 5). The copper rods withstood corrosion much better than the steel rods when UCO2 was used. Figure 7A,B shows the minor change on the surfaces of the copper rod before and after expose to UCO2. For up to three days, copper kept dissolving, but after that, the copper content remained constant.

Table 5. Measured copper concentration (ppm) after exposure to UCO2 for different times.

No. of Days	0	1	3	5	10
Cu (ppm)	<6	14.4 ± 0.4	25.3 ± 0.3	26.7 ± 0.5	25.8 ± 0.5

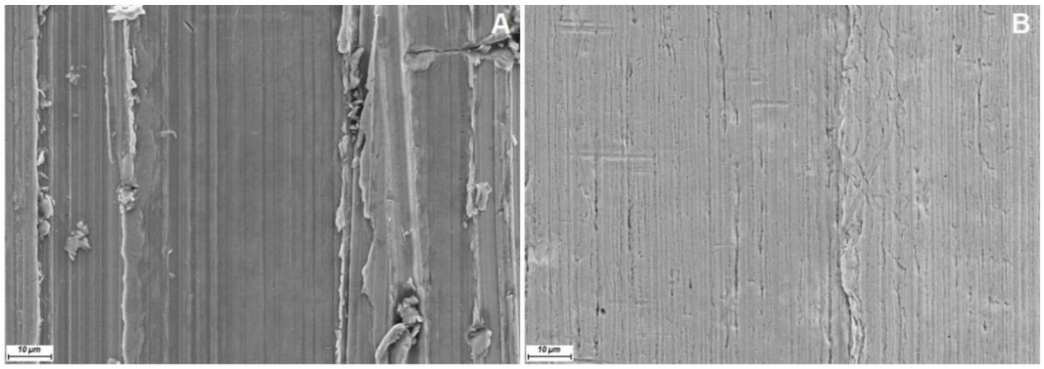

Figure 7. SEM secondary electron images of polished copper rod surfaces: (**A**) not exposed to the bio-oil and (**B**) exposed to UCO2 for 5 days.

The same batch of UCO2 was used in this copper test as in the test where UCO2 and UCO4 were mixed. A polished steel rod was used with UCO2 in the immersion test (3 d), and it was noticed that 277 ppm iron was dissolved into the oil (Figure 5).

When comparing the two rods in contact with the oil during the immersion test, the area 268.48 mm^2 of the polished copper rod was smaller compared to the polished steel rod's area of 431.57 mm^2. The concentration of copper dissolved from the rod was 0.09 ppm/mm^2, and the iron dissolved from the rod was 0.64 ppm/mm^2, which means that there was about 6.8 times higher concentration of iron compared to copper dissolved in UCO2 oil. These results indicate that the corrosive compounds in UCO2 caused more corrosion in contact with the polished steel rod surface compared to the copper rod surface.

Immersion tests with copper in UCOs could not be found in the open literature. Thus, we consider the corrosive properties of biodiesels for comparison. Biodiesel is chemically modified from UCOs and animal fats (that contain triglycerides and impurities like water, FFAs, etc.). During the chemical modification, including, e.g., transesterification, the production of biodiesel occurs, which is a mono-alkyl ester-based oxygenated fuel [34].

Immersion tests of copper, mild carbon steel, and stainless steel in biodiesel at 43 °C for two months were performed by Hu et al. [15]. According to their results, copper and mild carbon steel were observed to be more susceptible to corrosion than stainless steel. They also reported that chemical reactions controlled the corrosion mechanism of the metals [15]. Dissolved copper and iron were also found to act as strong catalysts to oxidize biodiesel [16]. Fazal et al. [9] also studied corrosion of copper in biodiesel and found out that after a certain immersion period (600–1200 h), the formation of oxygenated compounds on the surface of copper exposed to biodiesel reduced corrosion rate.

The immersion tests with biodiesel discussed above were done at elevated temperatures and for a longer immersion period [9,15,16,23,28]. During the biodiesel immersion

tests, copper was most vulnerable to corrosion; however, in our shorter period of immersion testing at room temperature with UCO2, polished copper was observed to be less corroded compared to the polished steel rod. The reason could be that the concentration of dissolved copper at room temperature reached a saturation level during the three-day immersion test, or there could be chemical reactions that control the corrosion of the copper surface exposed to the UCO2.

3.2.3. Corrosion Inhibitor

The immersion tests were made for three days with a polished steel rod and the bio-oil UCO2. During the test, there was 310 ppm iron dissolved in UCO2. Table 6 shows that when 0.025 wt% or 0.25 wt% tert-butylamine (TBA) was added to UCO2, the concentration of dissolved iron decreased to 9 ppm in both samples. When 2.42 wt% TBA was added to UCO2, the iron dissolved from the polished steel rod was 14 ppm. To prevent corrosion of a polished steel rod, 0.025 wt% TBA was enough to add to UCO2. The low iron concentration (9 ppm) measured in the bio-oil was on the same level as when no steel rod had been in contact with oil.

Table 6. The immersion test (3 d) with a polished steel rod and UCO2. TBA was added to the oil in different concentrations.

TBA (wt%)	0	0.025	0.25	2.42
Fe (ppm)	310	9	9	14

Deyab et al. [21] reported that corrosion inhibitors contain organic compounds with nitrogen, oxygen, or sulfur atoms, heterocyclic compounds, and pi electrons. The polar functional groups present in inhibitors are considered to be the center of reaction for adsorption [22]. Inhibitors ethylenediamine, tert-butylamine (TBA), or n-butylamine form a stable metal oxide protective layer and thus inhibit the corrosion in biodiesel [23]. Physical adsorption of amine-based inhibitors could have created a stable protective layer over the steel surface and thus prevented corrosion in our bio-oils [23,25].

As can be seen in Figure 8A,B, the steel rod surface after three-day immersion in UCO2 and TBA (0.025 wt%) is smoother than the immersion in UCO2 alone. The smoother surface observed when TBA was added originated from the smaller amounts of dissolved iron or less corrosion of the surface.

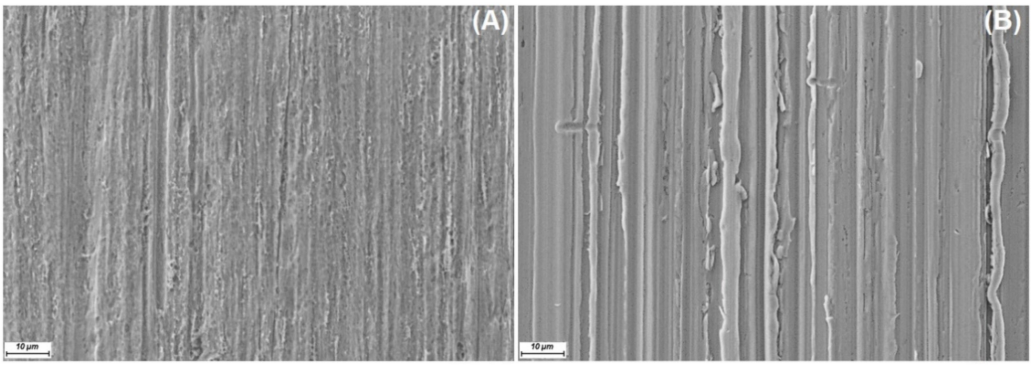

Figure 8. SEM secondary electron images of polished steel rod surfaces: (**A**) after exposure to UCO2 for 3 days and (**B**) after exposure to UCO2 and TBA (0.025 wt%).

Despite the promising results of TBA, notably inhibiting corrosion, it should be mentioned from the chemical safety point of view that it is classified as an acutely toxic substance. Therefore, more environmentally friendly chemicals as a replacement for TBA should be one of the focuses of future research in this area.

4. Conclusions

To study bio-oil-induced corrosion, unpolished and polished steel rods, polished mild annealed steel rods, and polished copper rods were immersed in vegetable-based used cooking oils at room temperature for up to 10 days. The iron content in the oils varied markedly depending on the oil sample. In general, the oils with the highest water concentrations (3100–3800 ppm) showed the highest corrosion properties although their acid number (AN) values of 6.7–6.9 mg KOH/g oil were not the highest. In contrast, the bio-oils with a lower level of water (2100–2700 ppm) but higher ANs (7–8.8 mg KOH/g oil) showed low corrosion properties. The oils with the highest ANs contained the highest concentrations of unsaturated free fatty acids, such as oleic acid. The unsaturated free fatty acids were assumed to have formed a protective layer on the rods, thereby preventing the permeation of oxygen and water to the metal surface. The copper rods withstood corrosion much better than the steel rods when UCO2 was used. For up to three days, copper kept dissolving, but after that, the copper content remained constant 25.9 ± 0.7 ppm. When a very corrosive oil was mixed with a non-corrosive oil, the amount of dissolved iron decreased notably. This suggests that mixing different bio-oils could be used as an advantage in corrosion prevention of fuel tanks and engines.

In the preliminary tests on the effect of corrosion inhibitors, it has been observed that adding even a very low concentration, 0.025 wt%, of TBA to the most corrosive used cooking oil clearly decreased the iron dissolution into the oil. Although more research needs to be carried out, the inhibiting effect could originate from the formation of a protective layer on the steel surface. However, due to the toxicity of TBA, more ecological alternatives should be studied.

Author Contributions: Conceptualization, N.B., L.H. and J.L.; methodology, N.B., L.H. and J.H.; formal analyses, N.B., J.H., L.H., J.L. and F.T.; investigation, N.B., L.H., J.L., J.H. and F.T.; writing—original draft, N.B.; writing—review and editing, F.T., L.H., J.L. and J.H.; supervision, L.H., J.L. and F.T.; project administration, N.B. and L.H.; funding acquisition, N.B. and L.H. All authors have read and agreed to the published version of the manuscript.

Funding: This research was funded by the Swedish Cultural Foundation in Finland and the Otto A. Malm Foundation. Authors are also grateful to the CircVol 6Aika project for financial support as part of the activities of the Johan Gadolin Process Chemistry Centre at Åbo Akademi University. The APC was funded by Åbo Akademi University.

Institutional Review Board Statement: Not applicable.

Informed Consent Statement: Not applicable.

Data Availability Statement: Data are contained within the article.

Acknowledgments: VG EcoFuel Oy is gratefully acknowledge for providing the oil samples.

Conflicts of Interest: The authors declare no conflict of interest.

References

1. Moretti, C.; Junginger, M.; Shen, L. Environmental life cycle assessment of polypropylene made from used cooking oil. *Resour. Conserv. Recycl.* **2020**, *157*, 104750. [CrossRef]
2. Van Grinsven, A.; van den Toorn, E.; van der Veen, R.; Kampman, B.; Oil, C. *Used Cooking Oil (UCO) as Biofuel Feedstock in the EU*; CE Delft: Delft, The Netherlands, 2020; p. 200247.
3. Panadare, D.C.; Rathod, V.K. Applications of waste cooking oil other than biodiesel: A review. *Iran. J. Chem. Eng.* **2015**, *12*, 55–76.
4. Chung, T.Y.; Eiserich, J.P.; Shibamoto, T. Volatile compounds identified in headspace samples of peanut oil heated under temperatures ranging from 50 to 200 °C. *J. Agric. Food Chem.* **1993**, *41*, 1467–1470. [CrossRef]
5. Wu, C.M.; Chen, S.Y. Volatile compounds in oils after deep frying or stir frying and subsequent storage. *J. Am. Oil Chem. Soc.* **1992**, *69*, 858–865. [CrossRef]
6. Singhabhandhu, A.; Tezuka, T. The waste-to-energy framework for integrated multi-waste utilization: Waste cooking oil, waste lubricating oil, and waste plastics. *Energy* **2010**, *35*, 2544–2551. [CrossRef]
7. Mannu, A.; Ferro, M.; DiPietro, M.E.; Mele, A. Innovative applications of waste cooking oil as raw material. *Sci. Prog.* **2019**, *102*, 153–160. [CrossRef]

8. Lhuissier, M.; Couvert, A.; Amrane, A.; Kane, A.; Audic, J.L. Characterization and selection of waste oils for the absorption and biodegradation of VOC of different hydrophobicities. *Chem. Eng. Res. Des.* **2018**, *138*, 482–489. [CrossRef]
9. Fazal, M.A.; Haseeb, A.S.M.A.; Masjuki, H.H. Corrosion mechanism of copper in palm biodiesel. *Corros. Sci.* **2013**, *67*, 50–59. [CrossRef]
10. Ollus, R.; Juoperi, K. Alternative fuels experiences for medium-speed diesel engines. In Proceedings of the 25th CIMAC Congress on Combustion Engine Technology, Vienna, Austria, 21–27 May 2007; International Council on Combustion Engines: Frankfurt, Germany, 2007; pp. 538–552.
11. Kovács, A.; Tóth, J.; Isaák, G.; Keresztényi, I. Aspects of storage and corrosion characteristics of biodiesel. *Fuel Process. Technol.* **2015**, *134*, 59–64. [CrossRef]
12. Rehioui, M.; Abbout, S.; Benzidia, B.; Hammouch, H.; Erramli, H.; Daoud, N.A.; Badrane, N.; Hajjaji, N. Corrosion inhibiting effect of a green formulation based on Opuntia Dillenii seed oil for iron in acid rain solution. *Heliyon* **2021**, *7*, e06674. [CrossRef] [PubMed]
13. Bruun, N.; Demesa, A.G.; Tesfaye, F.; Hemming, J.; Hupa, L. Factors affecting the corrosive behavior of used cooking oils and a non-edible fish oil that are in contact with ferrous metals. *Energies* **2019**, *12*, 4812. [CrossRef]
14. Fazal, M.A.; Haseeb, A.S.M.A.; Masjuki, H.H. Effect of temperature on the corrosion behavior of mild steel upon exposure to palm biodiesel. *Energy* **2011**, *36*, 3328–3334. [CrossRef]
15. Hu, E.; Xu, Y.; Hu, X.; Pan, L.; Jiang, S. Corrosion behaviors of metals in biodiesel from rapeseed oil and methanol. *Renew. Energy* **2012**, *37*, 371–378. [CrossRef]
16. Fazal, M.A.; Haseeb, A.S.M.A.; Masjuki, H.H. Comparative corrosive characteristics of petroleum diesel and palm biodiesel for automotive materials. *Fuel Process. Technol.* **2010**, *91*, 1308–1315. [CrossRef]
17. Alves, S.M.; Dutra-Pereira, F.K.; Bicudo, T.C. Influence of stainless steel corrosion on biodiesel oxidative stability during storage. *Fuel* **2019**, *249*, 73–79. [CrossRef]
18. Souza, C.A.C.; De Meira, M.; Assis, L.O.; De Barbosa, R.S.; Luna, S. Effect of natural substances as antioxidants and as corrosion inhibitors of carbon steel on soybean biodiesel. *Mater. Res.* **2021**, *24*, e20200234. [CrossRef]
19. Komatsu, D.; Souza, E.C.; De Canale, L.C.F.; Totten, G.E. Effect of antioxidants and corrosion inhibitor additives on the quenching performance of soybean oil. *Stroj. Vestn. J. Mech. Eng.* **2010**, *56*, 121–130.
20. Li, P.; Lin, J.; Tan, K.; Lee, J. Electrochemical impedance and X-ray photoelectron spectroscopic studies of the inhibition of mild steel corrosion in acids by cyclohexylamine. *Electrochim. Acta* **1997**, *42*, 605–615. [CrossRef]
21. Deyab, M.A. The inhibition activity of butylated hydroxytoluene towards corrosion of carbon steel in biodiesel blend B20. J. Taiwan Inst. *Chem. Eng.* **2016**, *60*, 369–375.
22. Deyab, M.A. Application of nonionic surfactant as a corrosion inhibitor for zinc in alkaline battery solution. *J. Power Source* **2015**, *292*, 66–71. [CrossRef]
23. Singh, B.; Korstad, J.; Sharma, Y.C. A critical review on corrosion of compression ignition (CI) engine parts by biodiesel and biodiesel blends and its inhibition. *Renew. Sustain. Energy Rev.* **2012**, *16*, 3401–3408. [CrossRef]
24. Yeşilyurt, M.K.; Öner, I.V.; Yilmaz, E.Ç. Biodiesel induced corrosion and degradation: Review. *Pamukkale Univ. Muh. Bilim. Derg.* **2019**, *25*, 60–70.
25. Fazal, M.A.; Sazzad, B.S.; Haseeb, A.S.M.A.; Masjuki, H.H. Inhibition study of additives towards the corrosion of ferrous metal in palm biodiesel. *Energy Convers. Manag.* **2016**, *122*, 290–297. [CrossRef]
26. Bruun, N.; Khazraie Shoulaifar, T.; Hemming, J.; Willför, S.; Hupa, L. Characterization of waste bio-oil as an alternate source of renewable fuel for marine engines. *Biofuels* **2022**, *13*, 21–30. [CrossRef]
27. Bruun, N.; Tesfaye, F.; Hemming, J.; Dirbeba, M.J.; Hupa, L. Effect of storage time on the physicochemical properties of waste fish oils and used cooking vegetable oils. *Energies* **2021**, *14*, 101. [CrossRef]
28. Zuleta, E.C.; Baena, L.; Rios, L.A.; Calderón, J.A. The oxidative stability and its impact on the deterioration of metallic and polymeric materials: A review. *J. Braz. Chem. Soc.* **2012**, *23*, 2159–2175. [CrossRef]
29. Karmakar, A.; Karmakar, S.; Mukherjee, S. Properties of various plants and animals feedstocks for biodiesel production. *Bioresour. Technol.* **2010**, *101*, 7201–7210. [CrossRef]
30. Gregg, F. *SVO: Powering Your Vehicle with Straight Vegetable Oil*; New Society Publishers: Gabriola Island, BC, Canada, 2008; pp. 29–79.
31. Adeoti, I.A.; Hawboldt, K. Comparison of biofuel quality of waste derived oils as a function of oil extraction methods. *Fuel* **2015**, *158*, 183–190. [CrossRef]
32. Swathi, P.N.; Rasheeda, K.; Samshuddin, S.; Alva, V.D.P. Fatty acids and its derivatives as corrosion inhibitors for mild steel—An overview. *J. Asian Sci. Res.* **2017**, *7*, 301–308. [CrossRef]
33. Guardia, P.; Batlle-Brugal, B.; Roca, A.G.; Iglesias, O.; Morales, M.P.; Serna, C.J.; Labarta, A.; Batlle, X. Surfactant effects in magnetite nanoparticles of controlled size. *J. Magn. Magn. Mater.* **2007**, *316*, e756–e759. [CrossRef]
34. Enweremadu, C.C.; Mbarawa, M.M. Technical aspects of production and analysis of biodiesel from used cooking oil—A review. *Renew. Sustain. Energy Rev.* **2009**, *13*, 2205–2224. [CrossRef]